Chapter 7

On Higher Order Resonant Periodic Orbits in the Photo–Gravitational Restricted Three–Body Problem

7.1 Introduction

A number of problems in space dynamics and astronomical systems can be solved using the techniques of restricted three–body problem (RTBP). Therefore, RTBP has received special significance in astrodynamics and astrophysics. The orbits of artificial satellite and spacecrafts are to be studied based on the theory of N–body problem. However, in many physical problems it can be approximated to three–body problem. For example, in the case of space missions from Earth to Moon or between two planets the technique of RTBP can be used. In such missions analytic and numerical techniques are used to solve the equations of motion developed in the framework of circular or elliptical RTBP.

The Kirkwood gap and the depletion of asteroid around Jupiter can be studied using RTBP and the theory of resonance. The stability of motion in the proximity of Lagrangian points bifurcates to two important cases: In the first case astroid population is expected around the triangular points as they are stable equilibrium points. In the second case we have the three unstable collinear equilibrium points, which are considered as repellent regions for the asteroid population. However, these points are suitable for transfer of spacecraft to a periodic orbit with the expense of the minimum energy. [Beutler (2004)], [Valtonen and Karttunen (2006)] have studied the stability of asteroid population using RTBP. Designing of quasi–periodic and periodic orbits around Lagrangian points have been carried out by [Markellos et. al. (1993)], [Dutt and Sharma (2011a)] [Abouelmagd (2012)], [Abouelmagd et. al. (2015)] and [Sosnitskii (2017)].

One of the most important contribution of RTBP is the Jacobi integral which can be used to construct the zero velocity curves, which enable us to determine the permitted regions of secondary body in space [Lukyanov (2009)] and [Abouelmagd and Mostafa (2015)]. Poincaré surface section (PSS) technique given by [Poincare (1892)] is a widely used technique for analyzing periodic and quasi–periodic orbits in a qualitative way. [Dutt and Sharma (2010)], [Dutt and Sharma (2011a)] have analyzed periodic orbits for Earth–Moon and Sun– Mars systems using PSS. [Pathak et. al. (2016a)], [Pathak and Thomas(2016b)] have used PSS technique to analyze periodic and quasi–periodic orbits for Sun–Saturn system with actual oblateness of Saturn and solar radiation pressure as perturbation. [Pathak and Thomas(2016b)] have studied stability analysis and separatrix analysis for different solar radiation pressure using PSS technique. [Pathak and Thomas (2016c)] and [Pathak and Thomas (2016d)] have analyzed periodic orbits around both primaries for Sun–Earth and Sun–Mars systems with oblateness and solar radiation pressure as the perturbation and have studied stability analysis using PSS. The PSS can be used to identify the periodic, quasi–periodic and chaotic regions in the phase space. Further, using Jacobi integral and PSS technique we can identify the order of resonance with the help of number of islands in the PSS.

7.1.1 Overview on resonance

The study of resonance has wide ranging applications in the solar system dynamics and theories related to satellite formation. It also plays an important role in the study of formation of rings around planets. A numerical relationship between frequencies or periods give rise to resonance. The resonance can be due to spin–orbit coupling or orbit–orbit coupling of two or more bodies. The reason for the moon always keeping its face towards the Earth is due to the spin–orbit resonance between them [Murray and Dermot (1999)]. It has been discussed by [Burns et. al. (1984)], that the thin ring around Jupiter is due to resonance in the magnetic field of the Jupiter with the motion of dust particles in its gravitational field.

Like the Earth–Moon system, majority of natural satellites of planets in the solar system are in synchronous spin–orbit resonance. The orbit–orbit resonance occurs among three of the major four satellites of Jupiter, known as Galilean satellites. More references in this regard are found in the works of [Henrard (1988)] and [Yoshikawa (1989)]. [Greenberg (1977)] and [Peale (1986)] have given useful reviews about orbital evolution through resonance. A large number of Trans–Neptunian objects (TNOs) having exterior order of resonance $2:3$ have received wide attention [Jewitt (1999)]. There are several objects having resonance close to the $1:2$, $1:3$ and $1:4$. In the Trans-Neptunian belt, stable regions close to resonant motion of TNOs is detected by [Morbidelli (1998), Yu and Tremaine (1999), Nesvorny and Roig (2001), Nesvorny and Roig (2000)].

On the PSS resonances can be detected with the help of number of islands. An extensive study on resonances has been done by [Morbidelli (1998)]. [Belbruno and Marsden (1997), Koon et. al.(2000)] have observed that in the motion of asteroids and comets, chaotic trajectories can be trapped around a resonance for a long time. [Tsiganis et. al. (2000)] have studied asteroids with autocorrelation time series function. [Ferraz–Mello et. al.(2003)] have analyzed existence of asymmetric libration and their importance for the stability of the $1:2$ and $1:3$ resonant motion in satellite and extra solar planetary systems. [Voyatzis and Kotoulas (2005)] have studied number of resonances associated with the dynamical features of Kuiper belt and located between 30 and 48 AU. This study was based on the computation of resonant periodic orbits and their stability. [Migliorini et al. (1998)] have studied the consequences higher order resonances $7:2$ and $10:3$ with Jupiter and resonances $4:7$, $5:9$, $7:2$ with Mars. [Morbidelli et. al. (1995)] have shown that some asteroid families are at higher order mean resonances 7:3 and 9:4. Outer asteroid belt also shows higher resonances of order $8:5$, $7:4$, and $9:5$, [Holman and Murray (1996)]. [Chiang et. al. (2004), Emel'yanenko and Kiseleva (2008)] have also shown that many of the Trans–Neptune objects (TNO) show higher order resonances $5:2$, $7:3$, $7:4$, and $9:5$. It was pointed out by [Thommes (2005)], that higher order resonances 5 : 2, 7 : 4, 9 : 5 have some role in the formation of planetary systems. [Balint et. al.(2012)] have studied the stability of higher order resonances in the restricted three body problem in which the primaries are the Sun–Jupiter and the Sun–Neptune systems. Asteroid belt and Saturn's ring are the results of interior resonance. The Saturnian system has widest variety of resonance phenomena [Murray and Dermot (1999)]. The Jupiter has a thin ring, which is thought to have been created by resonances. This resonance is due to numerical relationship between frequencies of motion of dust particle in Jupiter's gravitational field with rotation of the magnetic field of the planet [Burns et. al. (1984)]. [Contopoulos G. (1978)] have studied higher order resonance and they explained method of obtaining higher order resonant orbits by giving examples. Therefore it is pertinent to study the dynamics of higher order resonances. We have analyzed higher order interior resonant periodic orbits. We have obtained periodic orbits using PSS technique for the Sun–Earth and Sun–Mars systems incorporating solar radiation pressure and oblateness of second primary body as perturbing forces. The seventh, ninth and eleventh order interior resonant periodic orbits are analyzed for both Sun–Earth and Sun–Mars systems. The location, eccentricity and period of resonant orbits are investigated in the perturbed case for a given value of Jacobi constant C.

For the given order of resonance, period of the orbit is increased by exactly 6 or 7 units as number of loops is increased by 1, because the period of second primary body's orbit is 6.2827 units. It is observed that for the interior resonance as the number of loops increase, location of the periodic orbit moves away from the Sun. For the periodic orbit of the given number of loops, as the order of the resonance increases, location of periodic orbit moves towards Sun, whereas eccentricity and period decreases as order of resonance increases.

7.2 Model description

The equations of motion of the secondary body in the dimensionless synodic coordinates are given by equations (1.4.12) to (1.4.16). The expression for Jacobi constant C is given by equation (1.4.21). Mean motion n, oblateness coefficient A_2 and solar radiation pressure q are given by equations (1.4.17), (1.4.18) and (1.4.19), respectively. With the help of Eqs. (1.5.48) through (1.5.51) we can calculate the velocity

V, the angular momentum h , the semi–major axis a and the eccentricity e of the orbit of the secondary body.

For Sun-Planet system the period of planet in circular orbit is given by, $T_P = 2\pi/n$, where n is mean motion of the planet, which is given by Eq. (1.4.17). Indeed we will tabulate the relevant quantities such as: Jacobi constant C, obalteness coefficient A_2 , solar radiation pressure q, period of Earth T_E and its semi–major axis a_E , period of Mars T_M and its semi–major axes a_M in Table7.1.

Table 7.1: Some constants

C	A_2	q	a_E	T_E	a_M	T_M
2.93	0.0001	0.9845	1.0000011	6.2827	1.0003	6.2827

Equation (6.2.2) can be used to find the order of resonance, by finding the ratio between the semi–major axis of the infinitesimal body and the second primary body. Furthermore the number of islands in PSS also gives the order of resonance.

7.3 Interior seventh order resonance

We have analyzed seventh order resonance of periodic orbits in the perturbed Sun–Earth and the Sun–Mars systems. Numerical estimates of relevant quantities for seventh order interior resonance for the Sun–Earth and the Sun–Mars systems have been shown in Table 7.2 and Table7.3, respectively. Here the letters NL, LO, NI, RO, EC, TP and RP denote number of loops, location of the periodic orbit, number of islands, order of the resonance, eccentricity, time period of the orbit and ratio of the periods of the orbit, respectively.

The period of Earth's orbit is 6.2827 units. It can be noticed that as the number of loops increases successively from fifteen–loops to twenty two–loops, the period of the orbit of secondary body increases in such a way that the successive difference of periods differ either by 6 or 7 units as shown in Table 7.2. The period of fifteen–loops orbit is 51, while that of sixteen–loops orbit is 57 with a difference of 6 units. Also, period of Mar's orbit is 6.2827units. Order of resonance 15 : 8 shown in Table

7.3 indicates that $(a_1/a_2)^{(3/2)} = 2.01$ which is approximately $\frac{15}{8}$.

In a similar manner, it can be noticed that as the number of loops increases successively from fifteen–loops to twenty two–loops, the period of the orbit of secondary body increases in such a way that the successive difference of periods differ either by 6 or 7 units as shown in Table 7.3. Periodic orbit with fifteen–loops located at $x_0 = 0.35317$ is seventh order resonant orbit as its PSS gives seven islands as shown in Fig. 7.1(a). Magnified version of one of the islands is shown in Fig. 7.1(b). Number of loops varying from 15 to 20 and for 22–loops for Sun–Earth system are shown in Figs.7.2(a) – (g).

Fig.7.2(a) depicts 15–loops orbit. The orbit is symmetric about the line joining two primaries. The orbits with odd number of loops ranging from 15 to 19–loops are depicted in Figs.7.2(a), (c) and (e). These orbits are symmetric about the line joining the primaries (i.e. x–axis); but not about y–axis. While the orbits with even number of loops ranging from 16 to 20–loops and that with 22–loops are shown in Figs.7.2(b), (d), (f) and (g). These orbits are symmetric about both x and y–axes. It can be noticed that all the orbits are around the first primary and not orbiting the second primary. Further, it is observed that as the number of loops increase from 15 to 22, the over all size of the orbits increase.

Table 7.2: Analysis of interior seventh order resonance for perturbed Sun–Earth system

NL	LO	NI	RO	EC	TP	RP
15	0.35317		15:8	0.43754	51	2.09840
16	0.38844		16:9	0.40480	57	1.89674
17	0.41942		17:10	0.37783	63	1.80672
18	0.44597	7	18:11	0.35597	69	1.73540
19	0.47005		19:12	0.33711	76	1.67473
20	0.49084		20:13	0.32155	82	1.62506
22	0.52667		22:15	0.29626	94	1.54459

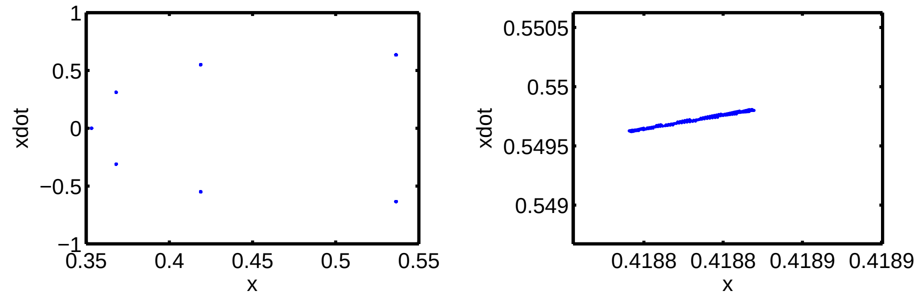

(a) PSS at $x_0 = 0.35317$. *(b) Enlarged PSS at $x_0 = 0.35317$.*

Figure 7.1: PSS of interior seventh order resonant fifteen–loops orbit when $q = 0.9845$, $A_2 = 0.0001$ and $C = 2.93$ for Sun–Earth system.

Table 7.3: Analysis of interior seventh order resonance for perturbed Sun–Mars system

NL	LO	NI	RO	EC	TP	RP
15	0.35315		15:8	0.43755	51	2.01083
16	0.38850		16:9	0.40474	57	1.89743
17	0.41928		17:10	0.37794	63	1.80794
18	0.44618	7	18:11	0.35579	69	1.73565
19	0.46995		19:12	0.33718	76	1.67574
20	0.49095		20:13	0.32146	82	1.62555
22	0.52650		22:15	0.29629	94	1.54568

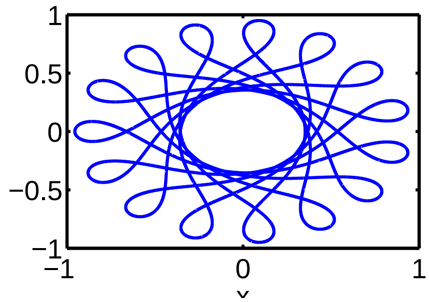

(a) Fifteen–loops orbit at $x_0 = 0.35317$.

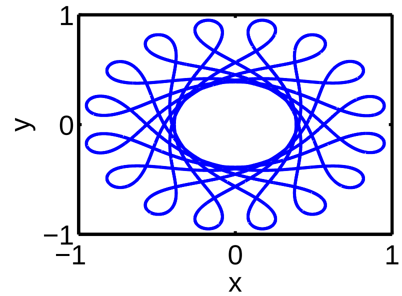

(b) Sixteen–loops orbit at $x_0 = 0.38844$.

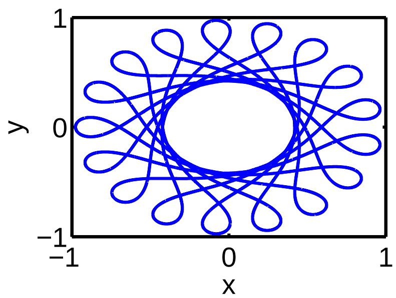

(c) Seventeen–loops orbit at $x_0 = 0.41942$.

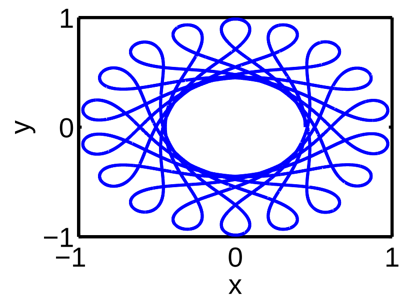

(d) Eighteen–loops orbit at $x_0 = 0.44597$.

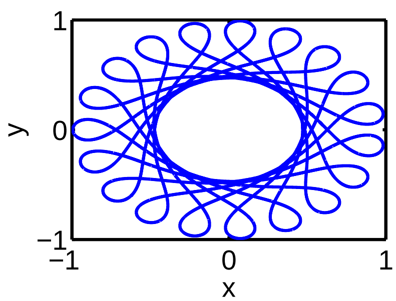

(e) Nineteen–loops orbit at $x_0 = 0.47005$.

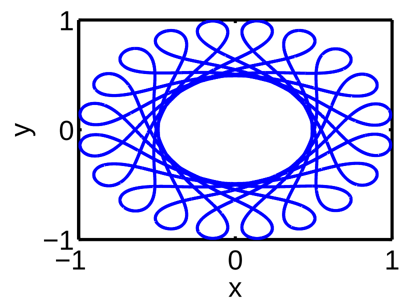

(f) Twenty–loops orbit at $x_0 = 0.49084$.

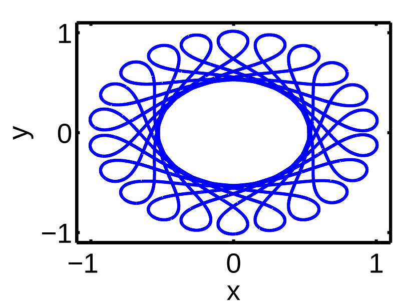

(g) Twenty two–loops orbit at $x_0 = 0.52667$.

Figure 7.2: Interior seventh order resonant orbits when $q = 0.9845$, $A_2 = 0.0001$ *and* $C = 2.93$ *for Sun–Earth system.*

7.4 Interior ninth order resonance

Numerical estimates of location, eccentricity, time period, ratio of time periods and other relevant quantities for ninth order interior resonance for Sun–Earth and Sun–Mars systems have been shown in Table 7.4 and Table 7.5, respectively. PSS of the twenty two–loops ninth order resonance of periodic orbit which is located at $x_0 = 0.42270$ is given in Fig.7.3(a). It shows nine islands which indicates this periodic orbit is ninth order resonant periodic orbit. Magnified version of one of the islands is shown in Fig.7.3(b).

Periodic orbits with number of loops 22, 23, 25 and 27 are shown in Figs.7.4(a)–(d). As in the case of seventh order resonant orbits, orbits with even number of loops are symmetric about both x and y–axes, while that with odd number of loops are symmetric about x–axis but not with respect to y–axis. The overall size of the orbit increases with number of loops.

Table 7.4: Analysis of interior ninth order resonance for perturbed Sun–Earth system.

NL	LO	NI	RO	EC	TP	RP
22	0.42270		22:13	0.37506	82	1.79764
23	0.44301	9	23:14	0.35835	88	1.74311
25	0.47915		25:16	0.33022	101	1.65270
26	0.49515		26:17	0.31840	107	1.61505

Table 7.5: Analysis of interior ninth order resonance for perturbed Sun–Mars system.

NL	LO	NI	RO	EC	TP	RP
22	0.42246		22:13	0.37526	82	1.79912
23	0.44334	9	23:14	0.35808	88	1.74305
25	0.47955		25:16	0.32991	101	1.65250
26	0.49530		26:17	0.31828	107	1.61545

7.5 Interior eleventh order resonance

Table 7.6 and Table 7.7 display numerical estimates of location, eccentricity, time period, ratio of time periods and other relevant quantities for eleventh order interior

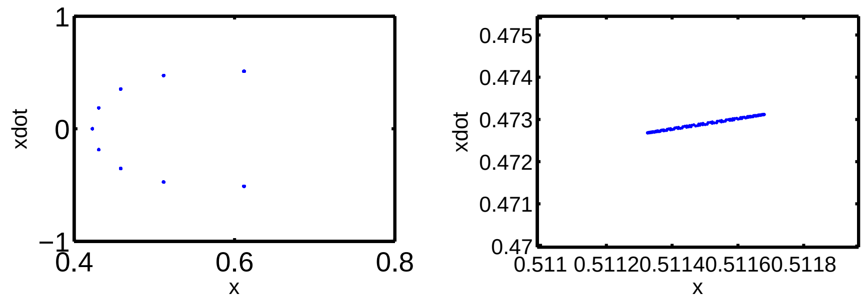

(a) *PSS at* $x_0 = 0.42270$. (b) *Enlarged PSS at* $x_0 = 0.42270$.

Figure 7.3: PSS of interior ninth order resonant twenty two–loops orbits when $q = 0.9845$, $A_2 = 0.0001$ *and* $C = 2.93$ *for Sun–Earth system.*

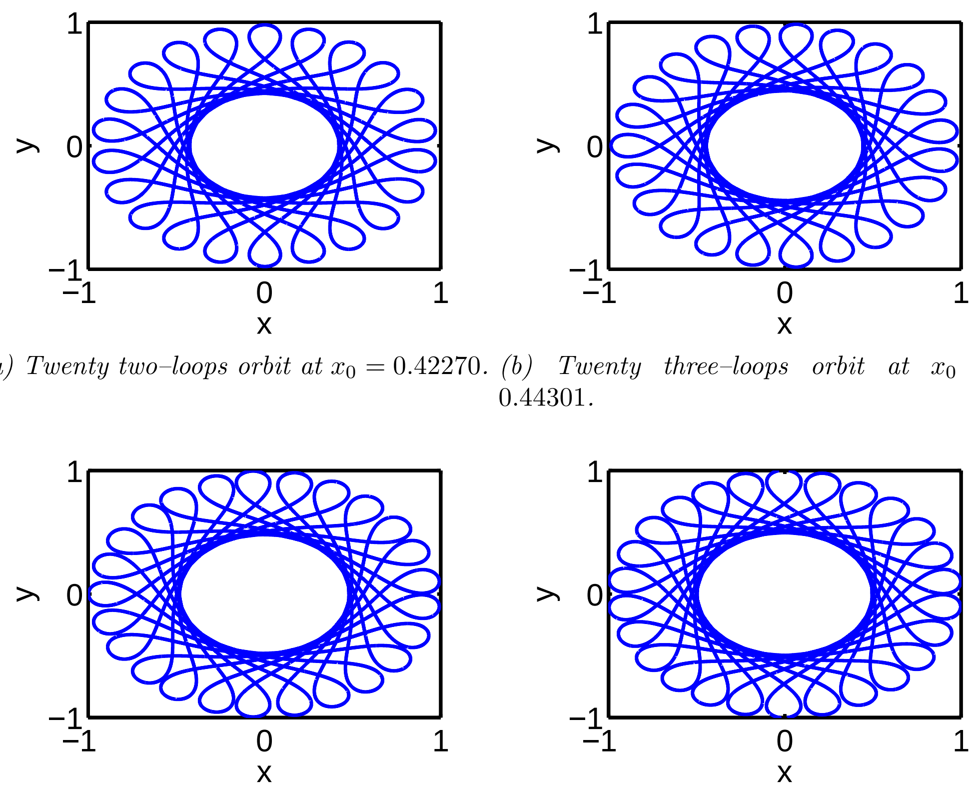

(a) *Twenty two–loops orbit at* $x_0 = 0.42270$. (b) *Twenty three–loops orbit at* $x_0 = 0.44301$.

(c) *Twenty five–loops orbit at* $x_0 = 0.47915$. (d) *Twenty six–loops orbit at* $x_0 = 0.49515$.

Figure 7.4: Interior ninth order resonant orbits when $q = 0.9845$, $A_2 = 0.0001$ *and* $C = 2.93$ *for Sun–Earth system.*

resonance for Sun–Earth and Sun–Mars systems, respectively. PSS of the twenty three–loops orbit of the eleventh order resonance is given in Fig.7.5(a), which is located at $x_0 = 0.33900$. The PSS shows eleven islands which indicates that the periodic orbit is eleventh order resonant periodic orbit. Magnified version of one of the islands is shown in Fig.7.5(b).

Periodic orbits with number of loops varying from 23 to 28–loops are shown in Fig.7.6(a)–(f). Orbits with odd number of loops as shown in Figs.7.6 (a), (c) and (f) are symmetric about $x-$axis only, while orbits with even number of loops are shown in Fig.7.6(b), (d) and (e) are symmetric about both x and y–axes. As in the case of seventh and ninth order of resonant orbits, the overall size of the orbits increase with increase in the number of loops. A noteworthy feature of all these high order resonant orbit is that they are about the first primary and secondary body never orbit the second primary. The distance between the second primary and the secondary body decreases as the number of loops increases.

Table 7.6: Analysis of interior eleventh order resonance for perturbed Sun–Earth system.

NL	LO	NI	RO	EC	TP	RP
23	0.339005		23:12	0.45133	76	2.05899
24	0.363215		24:13	0.42798	82	1.97635
25	0.385320	11	25:14	0.40760	88	1.90626
26	0.405935		26:15	0.38937	94	1.84494
27	0.424800		27:16	0.37330	101	1.79186
28	0.441035		28:17	0.35995	107	1.74829

Table 7.7: Analysis of interior ninth order resonance for perturbed Sun–Mars system.

NL	LO	NI	RO	EC	TP	RP
23	0.33898		23:12	0.45135	76	2.06002
24	0.36329		24:13	0.42791	82	1.97701
25	0.38548	11	25:14	0.40745	88	1.90664
26	0.40582		26:15	0.38946	94	1.84612
27	0.42446		27:16	0.37358	101	1.79362
28	0.44150		28:17	0.35956	107	1.74787

7.6 Effect of perturbing forces on physical and geometric parameters of higher order resonant orbits

The variation in the location of seventh, ninth and eleventh order resonant orbits for $C = 2.93$, $q = 0.9845$ and $A_2 = 0.0001$ in the Sun–Earth system is shown in Fig.7.7 against the number of loops of the periodic orbits. It can be noticed that the location of the orbit shifts towards the second primary body as the number of loops increases. It is observed from Fig.7.7 that both seventh and ninth order resonant orbits possess 22–loops. Further, it can be noticed that for a given number of loops, as the order of resonance increases, the location of the periodic orbits moves towards the Sun.

Similarly ninth and eleventh order resonant orbit admits orbit with 23– loops. Eleventh order resonant orbits admits 23–loops is nearer to Sun compared to ninth order resonant orbit with 23–loops. Seventh and ninth order resonance contains periodic orbit having 22–loops. From location of this orbit as shown in Fig.7.7, it is clear that for the given number of loops, as order of resonance increases location of periodic orbits moves towards the Sun. Similarly ninth and eleventh order resonance contains periodic orbit with 23–loops. Location of this orbit with eleventh order resonance is nearer to Sun in comparison of ninth order resonance.

The variation in the eccentricity of seventh, ninth and eleventh order resonant orbits

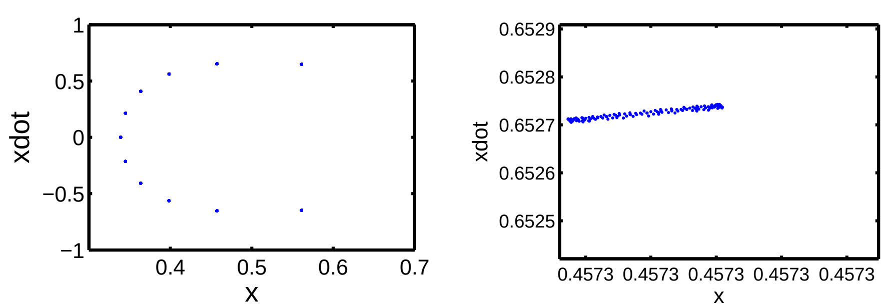

(a) PSS at $x_0 = 0.33900$. *(b) Enlarged PSS at $x_0 = 0.33900$.*

Figure 7.5: PSS of interior eleventh order resonant twenty three–loops orbits when $q = 0.9845$, $A_2 = 0.0001$ and $C = 2.93$ for Sun–Earth system.

for $C = 2.93$, $q = 0.9845$ and $A_2 = 0.0001$ for Sun–Earth system is shown in Fig.7.8 against the number of loops of the periodic orbits. It can be noticed that the eccentricity of the orbit decreases as the number of loops increases. From eccentricity of 22 and 23–loops orbits as shown in Fig.7.8, it is clear that for the given number of loops, as order of resonance increases eccentricity increases. The variation in the period of seventh, ninth and eleventh order resonant orbits for $C = 2.93$, $q = 0.9845$ and $A_2 = 0.0001$ for Sun–Earth system is shown in Fig.7.9 against the number of

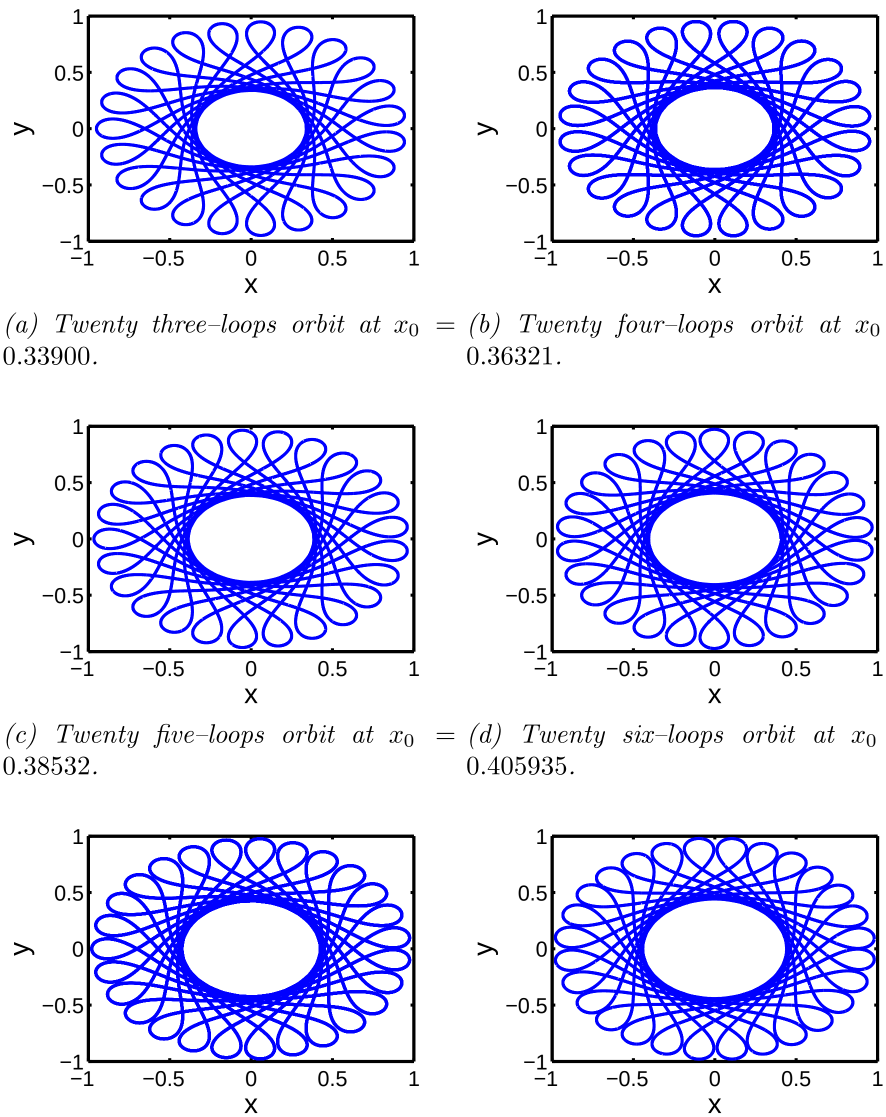

(a) Twenty three–loops orbit at $x_0 = 0.33900$.

(b) Twenty four–loops orbit at $x_0 = 0.36321$.

(c) Twenty five–loops orbit at $x_0 = 0.38532$.

(d) Twenty six–loops orbit at $x_0 = 0.405935$.

(e) Twenty seven–loops orbit at $x_0 = 0.42480$.

(f) Twenty eight–loops orbit at $x_0 = 0.44103$.

Figure 7.6: Interior eleventh order resonant orbits when $q = 0.9845$, $A_2 = 0.0001$ *and* $C = 2.93$ *for Sun-Earth system.*

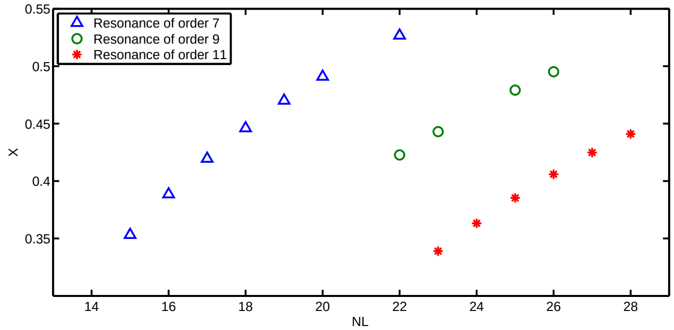

Figure 7.7: Variation in location of the interior seventh, interior ninth and interior eleventh order resonant periodic orbits when $q = 0.9845$*,* $A_2 = 0.0001$ *and* $C = 2.93$ *for Sun–Earth system.*

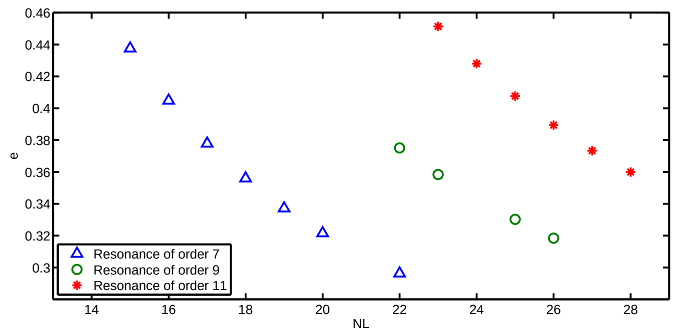

Figure 7.8: Variation in eccentricity of the interior seventh, interior ninth and interior eleventh order resonant periodic orbits when $q = 0.9845$*,* $A_2 = 0.0001$ *and* $C = 2.93$ *for Sun–Earth system.*

loops of the periodic orbits. From period of 22 and 23–loops orbits shown in Fig.7.9, it is clear that for the given number of loops, as order of resonance increases, the period decreases. Fig.7.10, Fig.7.11 and Fig.7.11 show similar results for the Sun–Mars system.

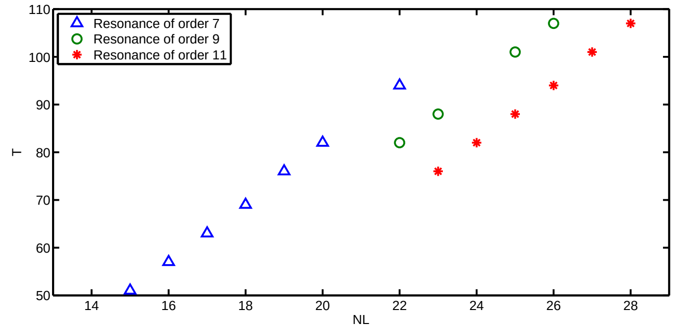

Figure 7.9: Variation in period of the interior seventh, interior ninth and interior eleventh order resonant periodic orbits when $q = 0.9845$, $A_2 = 0.0001$ and $C = 2.93$ for Sun–Earth system.

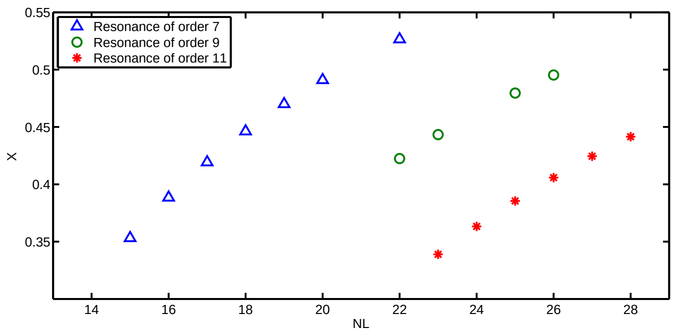

Figure 7.10: Variation in location of the interior seventh, interior ninth and interior eleventh order resonant periodic orbits when $q = 0.9845$, $A_2 = 0.0001$ and $C = 2.93$ for Sun–Mars system.

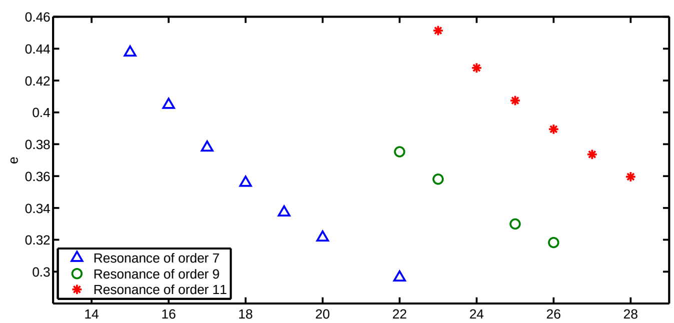

Figure 7.11: Variation in eccentricity of the interior seventh, interior ninth and interior eleventh order resonant periodic orbits when $q = 0.9845$, $A_2 = 0.0001$ and $C = 2.93$ for Sun–Mars system.

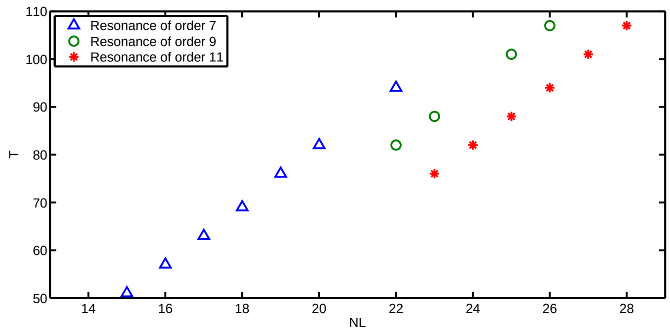

Figure 7.12: Variation in period of the interior seventh, interior ninth and interior eleventh order resonant periodic orbits when $q = 0.9845$*,* $A_2 = 0.0001$ *and* C *= 2.93 for Sun–Mars system.*

7.7 Conclusion

We have studied interior seventh, ninth and eleventh order resonances in the RTBP for Sun–Earth and Sun–Mars systems by considering the Sun as a radiating body and both Earth and Mars as oblate spheroids. It is observed that for the given order of resonance, period of the orbit is increased by exactly 6 or 7 units as number of loops is increased by 1 because period of the orbit of secondary body is 6.2827 units. It is concluded that for the interior resonance, as the number of loops increases, location of the periodic orbit moves away from the Sun.

Eccentricity of the periodic orbit decreases as number of loops increases for interior resonance in perturbed case. For the given order of resonance as perturbation increases eccentricity of the periodic orbit decreases. It is concluded that for the given number of loops, as order of resonance increases location of periodic orbits moves towards the Sun. Also, eccentricity of the orbit decreases as the number of loops increases. It can be observed that for the given number of loops, as order of resonance increases eccentricity increases. Period of the seventh, ninth and eleventh order resonant orbit increases as the number of loops increases. Further for a given number of loops, as order of resonance increases the period decreases.